

# Recyclable synthesis of isomaltulose using a whole-cell biocatalyst with robust sucrose isomerase

Mengkai Hu<sup>1</sup>, Fei Liu<sup>1</sup>, Zhi Wang<sup>1</sup>, Minglong Shao<sup>1</sup>, Meijuan Xu<sup>1</sup>, Taowei Yang<sup>1</sup>, Rongzhen Zhang<sup>1</sup>, Xian Zhang<sup>1</sup>, and Zhiming Rao<sup>1</sup>

<sup>1</sup>Jiangnan University

April 05, 2024

## Abstract

Sucrose isomerase (SI), catalysis sucrose to isomaltulose, has been widely used in industrial production of isomaltulose. Here, rational design of *Pantoea dispersa* SI for improving its thermostability by predicting and substituting the unstable amino acid residues was studied using the computational-aided predictor FoldX. Through the mutation pool, two mutants of SI (V280L, S499F) displayed favorable characteristics on thermostability. The double mutant V280L/S499F were further constructed and showed prolonged half-life at 45 °C, about 9-fold compared to the wild-type. Accordingly, the melting temperature of mutant V280L/S499F was improved to 54.2 °C. To determine the recyclable ability of mutant V280L/S499F to bioconversion of isomaltulose, recombinant *Corynebacterium glutamicum*/pXMJ19/pdsiV280L/S499F was constructed and repeated batch conversion was performed in a 5 L bioreactor. The results shown that the maximum yield of isomaltulose by batch conversion reached to 451 g/L with a productivity of 45.1 g/L/h, and the conversion rate remained  $83.2 \pm 2.1\%$  even after 15 repeated batches of biocatalysis. Structure-based molecule molding revealed that the interiors of mutant V280L/S499F was more tightly packed in a-9 fold and a new hydrophobic network was formed in a-17, which combined contributed to improving its thermostability. This work provides new reference for the sustainable production of isomaltulose.

## Recyclable synthesis of isomaltulose using a *Corynebacterium glutamicum* whole-cell biocatalyst with robust sucrose isomerase

Mengkai Hu<sup>1</sup>, Fei Liu<sup>1</sup>, Zhi Wang<sup>1</sup>, Minglong Shao<sup>1</sup>, Meijuan Xu<sup>1</sup>, Taowei Yang<sup>1</sup>, Rongzhen Zhang<sup>1</sup>, Xian Zhang<sup>1\*</sup>, and Zhiming Rao<sup>1\*</sup>

<sup>1</sup>Key Laboratory of Industrial Biotechnology of the Ministry of Education, School of Biotechnology, Jiangnan University, Wuxi, Jiangsu 214122, China

**Keywords:** Recyclable synthesis, isomaltulose, whole-cell biocatalyst, robust Sucrose isomerase

### \*Corresponding authors:

Dr. Xian Zhang, E-mail: [zx@jiangnan.edu.cn](mailto:zx@jiangnan.edu.cn), Tel:13771401977,

Prof. Zhiming Rao, E-mail : [raozhm@jiangnan.edu.cn](mailto:raozhm@jiangnan.edu.cn); , Tel:13921135816

### Abbreviations:

SI, Sucrose isomerase; DSF, Differential Scanning Fluorimetry; WT, Wild type enzyme; MD, molecular dynamic simulation; *C. glutamicum* 13032, *Corynebacterium glutamicum* ATCC13032 ; RMSD, Root mean square deviation; RMSF, root mean square fluctuation; IPTG, isopropyl- $\beta$ -D-thiogalactopyranoside;  $\Delta\Delta G$ , the relative folding free energy changes; SDS-PAGE, sodium dodecyl sulfate polyacrylamide gel electrophoresis; HPLC, high-performance liquid chromatography; RID, refractive index detector;  $T_m$  , melting temperature; VDW, Vander Waals forces.

## Abstract

Sucrose isomerase (SI), catalysis sucrose to isomaltulose, has been widely used in industrial production of isomaltulose. Here, rational design of *Pantoea dispersa* SI for improving its thermostability by predicting and substituting the unstable amino acid residues was studied using the computational-aided predictor FoldX. Through the mutation pool, two mutants of SI (V280L, S499F) displayed favorable characteristics on thermostability. The double mutant V280L/S499F were further constructed and showed prolonged half-life at 45 °C, about 9-fold compared to the wild-type. Accordingly, the melting temperature of mutant V280L/S499F was improved to 54.2 °C. To determine the recyclable ability of mutant V280L/S499F to bioconversion of isomaltulose, recombinant *Corynebacterium glutamicum*/ pXMJ19/*pdsi*<sup>V280L/S499F</sup> was constructed and repeated batch conversion was performed in a 5 L bioreactor. The results shown that the maximum yield of isomaltulose by batch conversion reached to 451 g/L with a productivity of 45.1 g/L/h, and the conversion rate remained 83.2 ± 2.1% even after 15 repeated batches of biocatalysis. Structure-based molecule molding revealed that the interiors of mutant V280L/S499F was more tightly packed in a-9 fold and a new hydrophobic network was formed in a-17, which combined contributed to improving its thermostability. This work provides new reference for the sustainable production of isomaltulose.

## Introduction

Isomaltulose, a sucrose isomer, is a reducing disaccharide that exists in natural molasses in a small amount and has a sweetness of 45% sucrose but is nontoxic and non-cariogenic.<sup>[1]</sup> Therefore, isomaltulose is an ideal sucrose substitute and is the healthy sugar certified by United States Food Drug Administration, its addition and consumption are not restricted.<sup>[2]</sup> In addition, isomaltulose has many beneficial healthcare functions and physiological properties, including inhibiting elevated blood sugar levels,<sup>[3]</sup> inhibiting fat accumulation,<sup>[4]</sup> improving anti-fatigue ability,<sup>[5]</sup> and maintaining the intestinal microecological balance.<sup>[6]</sup> However, the process of chemically synthesizing isomaltulose produces by-products and chemical waste, which increases the cost of product separation and wastewater treatment.<sup>[7]</sup> Therefore, the preparation of isomaltulose by biotransformation technology has been widely investigated in recent years.

Sucrose isomerase (SI, EC 5.4.99.11), also be known as isomaltulose synthase, is responsible for converting sucrose into isomaltulose or trehalulose along with glucose and fructose.<sup>[8]</sup> Current investigations of SI are mainly in the mining of novel genes and property characterizations of SIs. Those currently-reported SIs showed limited thermostability during the biocatalysis process, such as the SI of *Klebsiella* sp. LX3, which has a 1.8 min half-life at 50 °C,<sup>[9]</sup> SI of *Klebsiella pneumonia* lost its 40% relative activity after incubating at 50 °C for 20 min,<sup>[10]</sup> and SI of *Erwinia* sp. was completely inactive after incubating at 30 °C for 24 h.<sup>[11, 12]</sup> Although most studies have used enzyme immobilization or cell surface display technology to improve the robustness of SI, their industrial applications are still subject to unsatisfactory thermostability, and the conversion rate often decline rapidly after several continuous rounds of biocatalysis. Therefore, modification at the molecular level to improve the thermostability of SI should be further investigated.

Protein engineering has proven to be an effective approach to enhance thermostability of enzymes. Protein engineering is subdivided into directed evolution (irrational design), semi-rational design and rational design.<sup>[13]</sup> Although irrational design and semi-rational design were powerful in enzyme modification at elevated temperature,<sup>[14, 15]</sup> they are time-consuming and laborious. In contrast, rational design based on computer-aided techniques has greatly accelerated the speed and success rate of scientific research.<sup>[16]</sup> Fold X, one of the most reliable computational design predictors, has been developed to predict beneficial substitutions related to thermal stability by performing a rapid evaluation of the Gibbs free energy difference ( $\Delta\Delta G$ )<sup>[17, 18]</sup>. Recently, FoldX has been used to improve the thermostability of many enzymes by rational design. Luo *et al.* obtained a best variant PoOPH<sub>M9</sub> with a thermostability ( $T_{50}^{15}$ ) of 67.6 by hierarchical iteration mutagenesis using FoldX.<sup>[19]</sup> Bi *et al.* engineered thermophilic pullulanase by rational design using FoldX predictor, the  $T_m$  of mutant G692M increased by 3.8 °C, and half-life is 2.1-fold longer than the wild-type at 70 degC.<sup>[20]</sup> Wang *et al.* constructed a quadruple mutation (S142A/D217V/Q239F/S250Y) variant based on FoldX algorithm, the half-life of combination mutant increased 41.7-fold at 60 degC.<sup>[21]</sup> Thus, in-silico energy calculations (FoldX) may provide a clear guide for the molecular engineering of SI.

Compare with free-enzyme catalysis, while whole-cell biotransformation provides unique advantages, such as lower-cost preparation, easier separation of products and simpler recycle course. However, endotoxin or toxic cell wall pyrogens of non-food-grade host would be an obstacle to green synthesis of isomaltulose. To solve the potential safety hazards, some researchers have introduced SIase genes into non-pathogenic hosts, including *Lactococcus lactis* MG1363,<sup>[22]</sup> *B. subtilis* WB800,<sup>[23]</sup> *Saccharomyces cerevisiae*,<sup>[24]</sup> *Yarrowia lipolytica* S47.<sup>[25]</sup> However, recombinant *L. lactis* MG1363 exhibited low expression level of sucrose isomerase (100  $\mu\text{g}/\text{mL}$ ), and *Saccharomyces cerevisiae* and *Yarrowia lipolytica* grew slowly (48-96h). *Corynebacterium glutamicum* ATCC13032 (*C. glutamicum* 13032) is listed as a “generally recognized as safe” microorganism and has been successfully used as a host for producing food compounds efficiently, like amino acids, vitamins and organic acids and rare sugars.<sup>[26]</sup> Furthermore, *C. glutamicum* has many advantages and is superior to other food-grade strains, such as non-pathogenic, non-codon bias and short fermentation period. Thus, isomaltulose production by whole-cell biotransformation using an ideal food-grade host was expected to be more suitable in the field of food and fermentation research.

Herein, in order to obtain robust SI from a small mutation library via rational design, computational design software (FoldX5) coupled with conservation analysis and functional region assessment were employed to predict potential stabilizing point mutations. Then, the best variant was intracellular overexpressed in the food-grade strain *C. glutamicum* 13032, and the recombinant cells was further used as whole-cell biocatalyst for the recyclable synthesis of isomaltulose under the optimized conditions. Finally, Differential Scanning Fluorimetry (DSF) was used to evaluate the changes in the thermostability, and molecular dynamic simulation (MD) was used to elucidate the mechanism for the improved stability. Taken together, this study provides a new strategy for enhancing the stability of sucrose isomerase to improve its performance in industrial applications.

## Materials and methods

### 2.1 Reagents and enzymes

Sucrose, isomaltulose, HPLC-grade acetonitrile were bought from Aladdin (Shanghai, China). PrimSTAR Max DNA Polymerase, restriction enzymes, protein markers and *Dpn* I were obtained from TaKaRa (Dalian, China). Plasmid Mini Preparation Kit and BCA Protein Assay Kit were provided by Beyotime (Shanghai, China). Isopropyl- $\beta$ -D-thiogalactopyranoside (IPTG) and chloramphenicol was supplied by Yuanye Bio-Technology (Shanghai, China). All other reagents were purchased from Sinopharm Chemical Reagent (Shanghai, China) unless otherwise noted.

### 2.2 Plasmids, strains and medium

All strains and plasmids used in this study as shown in Table S1. The sequence of SI gene from the *Pantoea dispersa* UQ68J (*Pdsi*) (GenBank accession number: AY223549) without signal peptide was synthesized and sequenced by Suzhou GENEWIZ Company, and 6xHistag was added to the C-terminal of *Pdsi* for the protein purification. The *Pdsi* gene was incorporated in between *Hind* III and *EcoR* I site of the *E. coli*/*C. glutamicum* shuttle plasmid pXMJ19 to generate pXMJ19-*pdsi*. *E. coli* strain JM109 was used as gene cloning host to construct recombinant plasmids. *C. glutamicum* 13032 was used as expression host for the characterization of enzymatic properties and whole cells were used as biocatalysts for isomaltulose production. *E. coli* cells were cultured at 37 in LB medium (NaCl 10 g/L, peptone 10 g/L, yeast extract 5 g/L). *C. glutamicum* 13032 cells were grown on BHI medium at 30. 25  $\mu\text{g}/\text{mL}$  chloramphenicol was added when necessary.

### 2.3 Computational prediction for Sucrose isomerase thermostability

As starting point, the structure of WT and other mutants were modeled using the SI from *Erwinia rhapontici* NX5 (PDB: 4hph.1.A) as template with 74.10% sequence identity by SWISS-MODEL (<https://www.swissmodel.expasy.org>).<sup>[27]</sup> MolProbity<sup>[28]</sup> and PROCHECK<sup>[29]</sup> were applied for model evaluation, and evaluation results of WT are presented as Ramachandran plot (Fig S1). To identify the hot-spots for site-directed mutagenesis based on the  $\Delta\Delta G$  change, FoldX 3.0 algorithm was utilized to estimate the

folding free energy of SI. A standardized script written in python was performed to change all positions of the protein sequence to other 19 amino acids. The relative folding free energy changes ( $\Delta\Delta G = \Delta G_{\text{Mut}} - \Delta G_{\text{WT}}$ ) was calculated after each residue was mutated into the other amino acids.

## 2.4 Site-Directed Mutagenesis PCR

The plasmid pXMJ19-*psd* was used as amplification template to construct the SI mutants by using overlap extension PCR. Primers used are listed in Table S2. Final amplification fragments were digested by the endonuclease *Dpn* I at 37 for 1h, then the PCR mixture was chemically transformed into competent cells of *E. coli* JM109. The sequenced plasmids were transformed into *C. glutamium* 13032 by electroporation for protein expression.

## 2.5 Expression and Purification of the recombinant proteins

The recombinant *C. glutamium* 13032 strains were first cultivated into 10 mL BHI liquid medium supplemented with 25  $\mu\text{g}/\text{mL}$  chloramphenicol at 30 for overnight, and then 2% inoculation volume were transferred to 100 mL BHI medium containing 25  $\mu\text{g}/\text{mL}$  chloramphenicol at 30°C to an optical density @600nm of approximately 1 and induced by 1mM IPTG at 30°C for another 20 hours.

The cells were centrifuged ( $8000 \times g$ , 4) for 5 min and resuspended with 10 mL of 50 mM citric acid-sodium dihydrogen phosphate buffer (pH 6.0) after washing three times. The suspended cells were disrupted by sonication for 30 min and cells debris was discarded by centrifugation ( $8000 \times g$ , 4degC) for 30 min. The soluble supernatant fractions were first filtered and then further loaded onto a 1 mL Ni affinity column that was pre-equilibrated with 50 mM wash buffer (20 mM Tris and 500 mM NaCl, pH 7.4), and then elution buffer (20 mM Tris, 500 mM NaCl and 500 mM imidazole, pH 7.4) was used to elute the unbound proteins and SI with a linear gradient elution. Sodium dodecyl sulfate-polyacrylamide gel electrophoresis (SDS-PAGE) was used for analyzing purified protein. The concentration of protein was determined through Bradford method.

## 2.6 Enzyme assays

WT and its mutants were assayed for their isomaltulose-forming activity using 584 mM sucrose as substrate in 50 mM citric acid-sodium dihydrogen phosphate buffer (pH 6.0). Specifically, the reaction mixture consisting of 900  $\mu\text{L}$  of 584 mM sucrose solution and 100  $\mu\text{L}$  of purified enzymes in a final volume of 1 mL was incubated at 30°C for 10 min. The reaction was terminated by boiling the samples at 100 for 10 min. The isomaltulose production was quantified by high-performance liquid chromatography (HPLC). One unit (U) of enzyme activity was defined as the amount of enzyme that catalyzed the formation of 1  $\mu\text{mol}$  isomaltulose in 1 min under the described conditions.

## 2.7 Determination of optimal pH and temperature on enzyme activity

The optimal pH value for enzyme activity was assayed in 50 mM citric acid-sodium dihydrogen phosphate buffer (pH 4.0 to 8.0) at 30°C. The optimal temperature was determined between 20°C and 50°C in buffer (pH 6.0). To determine thermostabilities, the purified enzyme of WT and mutants were incubated at 45°C. The samples were taken every 20 min, and then the residual activity of WT and mutants after different incubation time was performed as described above. The original activity before incubating at 45°C was taken as 100%. Each assay was repeated three times.

## 2.8 Determination of Kinetic Parameters

Kinetic Parameters of these purified enzymes were determined under standard assay conditions with sucrose as a substrate. The sucrose substrate concentrations were as follows: 14.6, 29.2, 58.4, 102, 146, 234, 292 and 584 mM, respectively. Then,  $V_{\text{max}}$  and  $K_{\text{m}}$  values were determined through regression fitting of experimental data using GraphPad Prism 8.0.

## 2.9 Differential scanning fluorescence (DSF) assay

The DSF procedure used in this research was slightly modified according to previous report.<sup>[20]</sup> The  $T_m$  values were determined through monitoring the maximum relative fluorescence intensity after incubating the purified protein and SYPRO Orange dye together in PCR microplate at increasing temperatures in the real-time PCR machine.  $T_m$  values were measured in the range of 25~95°C at a rate of 1 °C/min. Three parallel samples were determined

## 2.10 Bioinformatics analysis

Molecular dynamic simulations (MD) were performed by using YASARA software (<http://www.yasara.org>). Specifically, the thermal fluctuations of WT and its mutant were analyzed by using an Amber03 force field, and SI was surrounded by H<sub>2</sub>O containing 0.29% NaCl with pH 6.0 in dodecahedron box. ConSurf Server (<https://consurf.tau.ac.il/>) was employed for identifying the functional regions of proteins.<sup>[30]</sup> Residue Interaction Network Generator (<http://old.protein.bio.unipd.it/ring/>) was used to recognize various kinds of interactions that introduced by the mutation in this study.<sup>[31]</sup> ESPript 3.0(<https://esript.ibcp.fr/ESPript/ESPript/>) was mainly employed for analysis of alignment sequence.<sup>[32]</sup>

## 2.11 HPLC analysis

Samples were determined by HPLC (Agilent 1260, USA) system equipped with a refractive index detector (RID) and separated by a NH<sub>2</sub> column (250 mm x 4.6 mm). The mobile phase was 80 % acetonitrile with the flow rate of 1.0 mL\*min<sup>-1</sup> at 30degC, and RID temperature was controlled at 35degC. The amounts of sugar concentration were calculated via peak areas.

## Results and Discussion

### 3.1 Selection of the mutagenesis sites for improving thermostability of sucrose isomerase

In order to rationally design the most promising mutants, we used FoldX to screen natural hot spots that may be related to thermostability.  $\Delta\Delta G$  values of all 10982 possible single point mutations were first calculated to predict the possibility of point mutations affecting protein thermostability. Among them, the mutation site with  $\Delta\Delta G > 0$  will be excluded. To further improve the prediction accuracy by the FoldX algorithm, an additional conservation analysis was performed to avoid point mutations that would lead to loss of enzyme activity.<sup>[33]</sup> The amino acid marked with f or s was highly conserved amino acid and further excluded (Figure S2). Finally, 10 point mutations were selected for the next experimental study: E76R, A100E, G152P, I205M, V280L, S328F, S499F, S563R, S563L, N578M (Table 1). The distribution of the mutation points is shown in the Figure 1A.

To test whether these substitution mutations improved the thermostability of SI, each single point mutation was individually expressed in *C. glutamium* 13032 (Figure 1B). The thermostability of mutants was evaluated by determining the residual activity of enzyme after heat treatment at 45°C for 20 min. As shown in Figure 1C, WT retained 15.7% of its initial activity, whereas two positive mutants V280L, and S499F retained 49.1% and 43.2% of their individual original activity, respectively. However, the thermostability of other mutants did not change or decreased significantly. These results demonstrated that V280L and S499F show better thermostability than WT. To assess the possible interaction between these two single point mutations, double mutant V280L/S499F was further constructed and investigated. V280L/S499F retained 93.3% of its initial activity after incubating at 45°C for 20 min.

### 3.2 Enzymatic properties and Kinetic Analysis of mutants

The thermostabilities and catalytic properties of the WT and mutants were further characterized. The optimal pH value of three mutants was 5.5, which was similar to that of the WT (Figure 2A). Consistent with WT, the optimal temperature of these three positive mutants were also 30°C, while they exhibited higher relative activity at the same temperature (Figure 2B). At 45°C, WT retained 58.1% of its maximum activity, whereas mutants V280L, S499F and V280L/S499F retained 61.8%, 59.4%, and 74.1% of its maximum activities, respectively.

Then, we evaluated the changes in thermostability by assessing residual activities of these three mutants and WT after different incubation times at 45°C. As shown in Figure 2C, the thermostability of mutants was better than that of WT, and V280L/S499F displayed the greatest improvement in thermostability. At 45°C, the  $t_{1/2}$  of WT was 11.2 min. In contrast, the  $t_{1/2}$  of V280L, S499F and V280L/S499F were 25.4, 21.5 and 100 min, which are 2.26, 1.91 and 8.9 times better than that of WT. These findings thus indicated that two of amino acid substitutions (V280L and S499F) were beneficial to improve thermostability of SI.

Kinetic parameters of the WT and its mutants were measured using different concentrations of sucrose as substrate. As listed in Table 1, three mutants showed little differences in catalytic activity with WT.  $K_m$  and  $k_{cat}/K_m$  of these mutants also changed slightly, indicated that point mutations has little influence on enzyme properties while improving the thermostability.

To further evaluate thermodynamic stability of WT and its variants, melting temperature ( $T_m$ ) was measured by DSF. As shown in Figure 2D, the  $T_m$  of WT was 50.6°C, while the  $T_m$  values of V280L, S499F, and V280L/S499F mutants was 52.7, 51.8 and 54.2°C, respectively. These results are consistent with the thermostability studies of the three positive mutants.

### 3.3 Optimization of reaction conditions for whole-cell biotransformation

Outstanding thermostability of SI has always been pursued in successful industrial manufacturing bioprocess for isomaltulose, as even slight enhancement can improve long-term activity under optimum conditions, increase the ability to remain high activity in repeat batches of whole-cell biotransformation. To develop an economically feasible whole-cell biocatalysis process, the influence of temperature, pH, cell density as variables were explored. As shown in Figure 3A, the optimum pH of whole-cell activity was 6.0, which was higher than that of pure enzyme expressed from *C. glutamicum*. Wu's report also showed the same shift in the optimal pH, which may be attributed by the differences of micro-environment.<sup>[23]</sup> Whereas no obvious changes were detected in the optimum temperature between free enzyme and whole-cell activity, all the maximum catalytic activity was at 30 (Figure 3B). Moreover, cell dosage also plays an important in the actual production, and reaction time is related to the cell density during the biotransformation process. Figure 3C shows that the concentration of isomaltulose was highest in the first 1.5 h when the cell density was  $OD_{600}=30$ , while the yield of isomaltulose at  $OD_{600}=25$  was significantly higher than  $OD_{600}=30$  after 1.5 h. Therefore,  $OD_{600}=25$  was selected as the optimal cell dosage for the synthesis of isomaltulose.

### 3.4 Recyclable synthesis of isomaltulose under optimized conditions in 5 L fermenter

Based on the above results, one-batch whole-cell biocatalysis process was applied to *C. glutamicum* /pXMJ19/*pdsi*<sup>V280L/S499F</sup> cells to transform sucrose to isomaltulose in a 5 L fermenter. The other details were as follows: reaction volume 2 L, rotational speed 200 r.min<sup>-1</sup>, 1X-100, and 500 g/L sucrose as substrate. The reaction time-course curves, consisting of isomaltulose production, as well as by-product glucose and fructose accumulation, are illustrated in Figure 3D. The concentration of isomaltulose increased rapidly for the first 6 h and gradually reached a plateau after 10 h. Specifically, the maximum yield of isomaltulose reached 451 g.L<sup>-1</sup> in 10 h with a conversion rate of 90.2% (w/w) and a productivity of 45.1 g/L/h. At the same time, 7.2 ± 1.5 g/L of glucose and 10.6 ± 0.8 g/L of glucose fructose were concurrently produced as a byproduct during the reactions.

To increase isomaltulose productivity and save the cost of culturing bacteria, continuous catalytic reaction of recombinant cells was evaluated by measuring the conversion rate of 500 g/L sucrose in a 5 L fermentor biotransformation system. As depicted in Figure 3E, the whole-cell *C. glutamicum* /pXMJ19/*pdsi*<sup>V280L/S499F</sup> exhibited robust and great operational stability by reaching a total reaction batches of 180 h (every batch took 12 h, including 2 h for substrate preparation and cell collection) and maintaining more than 83.2 ± 2.1% of the initial isomaltulose productivity even after 15 batches of repeated utilization at 30 degC, but the conversion rate of WT decreased 63.3 ± 1.6% after 15 batches. Wu and Li also reported the use of *B. subtilis* and *Yarrowia lipolytica* as whole-cell biocatalyst to synthesize isomaltulose respectively, while the conversion rate dropped to about 80% after 12 batches of biotransformation.<sup>[26, 28]</sup> Therefore, we successfully obtained a recombinant GRAS strain, which had the highest operational stability, and the productivity was also the

highest reported in food-grade strains to date (details listed in the Table S3).

### 3.5 Structure analysis of mutant enzymes for improving thermostability

To analyze the conformational change of the mutations caused by each substituted residue, three-dimensional structure of WT and mutants were homology modeled with Swiss-Model protein automated modeling program.

The tight packing of protein interiors plays a vital role in protein stability for the burial of both polar and nonpolar groups, and one  $-CH_2-$  group is buried on folding contributes 1.1  $\pm$  0.5 kcal/mol of energy to protein stability.<sup>[34]</sup> As shown in Figure 4A, a single  $-CH_2-$  group was added to side chain after mutating the amino acid Val to Leu at position 280. This seems to reveal that the introduction of alanine's bulky non-polar side chain may be responsible for improving the stability. In addition, inspection of the structure model of the V280L showed that L280 were located in the  $\alpha$ -helix (Figure 4B), and V280L substitution also generated two Vander Waals forces (VDW) bonds with Q329 and T330 of the other  $\alpha$ -helix. Therefore, the two newly introduced VDW may also stabilize the local stability, thereby facilitate the geometry more stable. The same strategy was also applied to improve the thermostability of *Bacillus thermoleovorans* pullulanase successfully.<sup>[20]</sup> More interestingly, we were surprised to find that all the amino acids at 280 sites from other sources were L except for V from the *Pantoea dispersa* UQ68J through multiple sequence alignment Figure 4C. Therefore, the improvement of thermostability of V280L mutant may also be related to the evolutionary conservatism of the enzyme.<sup>[35]</sup>

Previous studies have pointed out that molecular interactions, including hydrogen bonds, disulfide bonds, VDW, aromatic–aromatic interaction, and hydrophobic interaction are the major structural factors that take effect on the protein thermostability. In all of these factors, the contribution of hydrophobic interaction to protein stability accounts for about 60%.<sup>[36]</sup> As shown in Figure 4E, a new hydrophobic network formed for substituted residue from hydrophilic S (Figure 4D) to strong hydrophobic F at the site 499, which contains four residues (P24, W339, P495, and L519) within 5 angstroms. Therefore, the residue 499 greatly changed the hydrophobic stacking around the mutation, thereby enhancing the hydrophobic interaction effect. In addition, a cation– $\pi$  interaction between F499 and W339 was found after mutation, which may further improve the thermostability of mutant S499F. In summary, the improved thermostability of mutant S499F may be the result of the hydrophobic interactions and cation– $\pi$  interaction. Moreover, there were no new molecular interactions being introduced into the double mutant V280L/S499F (Figure 4F), maybe the synergistic effect of these two single point mutations further promoted the improvement of stability of the double mutant.

### 3.6 MD simulation analysis for improved thermostability

In order to further clarify the overall structural rigidity of enzyme and the fluctuation changes of each amino acid residue, we conducted MD of WT and three mutants (V280L, S499F, V280L/S499F) at 318K for 30ns in this study. Root mean square deviation (RMSD) and root mean square fluctuation (RMSF) are used to represent the degree of molecular structure change and freedom of movement of individual atoms in a molecule respectively. As shown in Figure 5A, the RMSD of all systems no longer fluctuates drastically after 13 ns, and then RMSD varied around 1.5 nm. After equilibration at 318 K, the average values of WT was 1.659 nm, whereas the average values of three mutants (V280L, S499F, V280L/S499F) declined to 1.457 nm, 1.520 nm and 1.353 nm, respectively. Since the thermostability of protein is not positively correlated with its RMSD value, the lower RMSD value of mutants indicated the mutated structure was relative stable than that of the WT.

Similarly, RMSF could also reflect the local flexibility of protein. The higher RMSF value of one region, indicating that conformation of this region was more unstable. As shown in Figure 5B, some regions around residue V280, S499 showed great fluctuations in RMSF values of WT at 318 K. Generally, these amino acids were thought to be thermo-unstable. On the contrary, RMSF of three mutants (V280L, S499F, V280L/S499F) showed mild fluctuations in the same areas of WT mentioned above. In conclusion, mutations in these sites (V280, S499) contribute greatly to improve the stability of SI.

## Concluding remarks

In this work, the thermal stability of SI from *Pantoea dispersa* UQ 68J toward sucrose isomerization was greatly improved via rational engineering by utilizing computer-aided design coupled with conservation analysis and functional region assessment. We obtained a robust variant V280L/S499F, displayed a 3.6 increase in apparent melting temperature, an 8.9-fold longer of half-life at 45 . Moreover, the recombinant *C. glutamicum* /pXMJ19/*pdsi*<sup>V280L/S499F</sup> whole-cell exhibited robust and the continuous operational stability for recyclable synthesis of isomaltulose, the conversion rate remained  $83.2 \pm 2.1\%$  even after 15 continuous rounds of biocatalysis. More importantly, we further characterized the reason underlying increased thermostability in detail. These results showed that the comprehensive strategies are a universal and efficient method that can improve the thermostability of enzyme without a lot of experiment.

## Conflict of interest

The authors declare no conflict of interest in part or full during and after this study.

This article does not contain any studies with human participants or animals performed by any of the authors.

## Acknowledgement

This work was supported by the National Key Research and Development Program of China, (No. 2020YFA0908300), National Natural Science Foundation of China (No. 32071470), Key Research and Development Project of Shandong Province, China (No. 2019JZZY020605), the Project Supported by the Foundation of State Key Laboratory of Biobased Material and Green Papermaking, Qilu University of Technology, Shandong Academy of Sciences (No. KF201907), the Postgraduate Research & Practice Innovation Program of Jiangsu Province (KYCX21\_2026).

## References

- [1] M. Barea-Alvarez, M. T. Benito, A. Olano, M. L. Jimeno, F. J. Moreno, *Journal of agricultural and food chemistry*, **2014** , *62* , 9137-9144.
- [2] B.A.R. Linaa, D. Jonkera, G. Kozianowskib, *Food and Chemical Toxicology*, **2002** , *40* , 1375-1381.
- [3] C. C. Maresch, S. F. Petry, S. Theis, A. Bosy-Westphal, T. Linn, *Nutrients*, **2017** , *9* .
- [4] S. J. Lee, W. K. Yu, H. R. Park, H. Kim, J. H. Kim, J. Park, K. S. Shin, *J Food Biochem*, **2020** , *44* , e13201.
- [5] E. J. Stevenson, A. Watson, S. Theis, A. Holz, L. D. Harper, M. Russell, *European journal of applied physiology*, **2017** , *117* , 2321-2333.
- [6] F. E. Kendall, O. Marchand, J. J. Haszard, B. J. Venn, *Nutrients*, **2018** , *10* .
- [7] W. Zhang, T. Zhang, B. Jiang, W. Mu, *Biotechnol Adv*, **2017** , *35* , 267-274.
- [8] W. M. Mu, W. J. Li, X. Wang, T. Zhang, B. Jiang, *Appl Microbiol Biot*, **2014** , *98* , 6569-6582.
- [9] S. Li, H. Cai, Y. Qing, B. Ren, H. Xu, H. Zhu, J. Yao, *Appl Biochem Biotechnol*, **2011** , *163* , 52-63.
- [10] A. Aroonmual, T. Nihira, T. Seki, W. Panbangred, *Enzyme Microb Tech*, **2007** , *40* , 1221-1227.
- [11] H. Y. Kawaguti, H. Harumi Sato, *Appl Biochem Biotechnol*, **2010** , *162* , 89-102.
- [12] H. Y. Kawaguti, H. H. Sato, *Food Chem*, **2010** , *120* , 789-793.
- [13] V. Stepankova, S. Bidmanova, T. Koudelakova, Z. Prokop, R. Chaloupkova, J. Damborsky, *Acs Catal*, **2013** , *3* , 2823-2836.
- [14] P. A. Tizei, E. Csibra, L. Torres, V. B. Pinheiro, *Biochem Soc Trans*, **2016** , *44* , 1165-1175.

- [15] F. H. Arnold, *Angewandte Chemie*, **2019** ,58 , 14420-14426.
- [16] H. Cui, H. Cao, H. Cai, K. E. Jaeger, M. D. Davari, U. Schwaneberg, *Chemistry*, **2020** , 26 , 643-649.
- [17] R. Guerois, J. E. Nielsen, L. Serrano, *Journal of Molecular Biology*, **2002** , 320 , 369-387.
- [18] J. Schymkowitz, J. Borg, F. Stricher, R. Nys, F. Rousseau, L. Serrano, *Nucleic Acids Res*, **2005** , 33 , W382-388.
- [19] X. J. Luo, J. Zhao, C. X. Li, Y. P. Bai, M. T. Reetz, H. L. Yu, J. H. Xu, *Biotechnology and bioengineering*, **2016** ,113 , 2350-2357.
- [20] J. Bi, S. Chen, X. Zhao, Y. Nie, Y. Xu, *Appl Microbiol Biotechnol*, **2020** , 104 , 7551-7562.
- [21] R. Wang, S. Wang, Y. Xu, X. Yu, *International journal of biological macromolecules*, **2020** , 160 , 1189-1200.
- [22] J. Y. Park, J. H. Jung, D. H. Seo, S. J. Ha, J. W. Yoon, Y. C. Kim, J. H. Shim, C. S. Park, *Bioresour Technol*, **2010** ,101 , 8828-8833.
- [23] L. Wu, S. Wu, J. Qiu, C. Xu, S. Li, H. Xu, *Food Chem*,**2017** , 229 , 761-768.
- [24] G. Y. Lee, J. H. Jung, D. H. Seo, J. Hansin, S. J. Ha, J. Cha, Y. S. Kim, C. S. Park, *Bioresource Technol*, **2011** ,102 , 9179-9184.
- [25] L. J. Li, H. W. Wang, H. R. Cheng, Z. X. Deng, *J Funct Foods*, **2017** , 32 , 208-217.
- [26] K. C. Shin, D. H. Sim, M. J. Seo, D. K. Oh, *Journal of agricultural and food chemistry*, **2016** , 64 , 8146-8153.
- [27] Z. Xu, S. Li, J. Li, Y. Li, X. Feng, R. Wang, H. Xu, J. Zhou, *Plos One*, **2013** , 8 , e74788.
- [28] V. B. Chen, W. B. Arendall, 3rd, J. J. Headd, D. A. Keedy, R. M. Immormino, G. J. Kapral, L. W. Murray, J. S. Richardson, D. C. Richardson, *Acta crystallographica. Section D, Biological crystallography*, **2010** , 66 , 12-21.
- [29] R. a. L. M. W. M. D. S. M. J. M. Thornton. *Journal of Applied Crystallography*, **1993**, 26(2)
- [30] C. Berezin, F. Glaser, J. Rosenberg, I. Paz, T. Pupko, P. Fariselli, R. Casadio, N. Ben-Tal, *Bioinformatics*, **2004** ,20 , 1322-1324.
- [31] D. Piovesan, G. Minervini, S. C. Tosatto, *Nucleic Acids Res*, **2016** , 44 , W367-374.
- [32] X. Robert, P. Gouet, *Nucleic Acids Res*, **2014** ,42 , W320-324.
- [33] G. Li, X. Fang, F. Su, Y. Chen, L. Xu, Y. Yan, *Appl Environ Microbiol*, **2018** , 84 , e02129-17.
- [34] C. Nick Pace, J. M. Scholtz, G. R. Grimsley, *Febs Lett*,**2014** , 588 , 2177-2184.
- [35] M. M. Pinney, D. A. Mokhtari, E. Akiva, F. Yabukarski, D. M. Sanchez, R. Liang, T. Doukov, T. J. Martinez, P. C. Babbitt, D. Herschlag, *Science*, **2021** , 371 .
- [36] M. M. Gromiha, M. C. Pathak, K. Saraboji, E. A. Ortlund, E. A. Gaucher, *Proteins*, **2013** , 81 , 715-721.

## TABLES AND FIGURES

**Table 1.** The  $\Delta\Delta G$  values of candidate mutants computed by FoldX

Position	Original amino acid	Mutant amino acid	$\Delta\Delta G$ value (Kcal* $\text{mol}^{-1}$ )
76	E	R	-1.94251
100	A	E	-1.17737

Position	Original amino acid	Mutant amino acid	$\Delta\Delta G$ value (Kcal* $\text{mol}^{-1}$ )
152	G	P	-2.26873
205	I	M	-1.43737
280	V	L	-1.68313
328	S	F	-2.41961
499	S	F	-1.57516
563	S	L	-1.53936
563	S	R	-1.57516
578	N	M	-1.41972

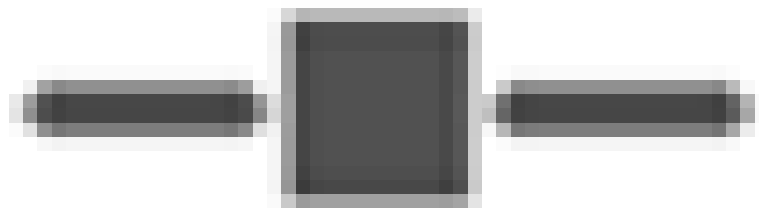
**Table2.** Comparison of wild-type and mutants enzymatic properties

Enzyme	$K_m$ (mM)	$K_{cat}$ ( $\text{S}^{-1}$ )	$K_{cat}/K_m$ ( $\text{S}^{-1}\text{mM}^{-1}$ )	$T_m$ ( $^{\circ}$ )	$t_{1/2}$ (min) (45)	Special activity (U $\text{mg}^{-1}$ )
Wild-type	42.1 $\pm$ 1.8	712 $\pm$ 6.1	16.7	50.6	11.2	627
V280L	44.1 $\pm$ 2.1	698 $\pm$ 7.2	15.8	52.7	25.4	615
S499F	43.2 $\pm$ 1.5	701 $\pm$ 6.8	16.2	51.8	21.5	620
V280L/S499F	42.8 $\pm$ 1.7	708 $\pm$ 6.5	16.5	54.2	100	623

### Figure legends

**Figure 1.** (A) Distribution of the mutations in protein PDSI. The residues at the mutational sites are shown as spheres. (B) SDS-PAGE shows the expression of mutants. Lane M, protein marker; Lane1, *C. glutamicum* /pXMJ19/pdsiWT; Lane2-12, *C. glutamicum* /pXMJ19/pdsi (E76R, A100E, G152P, I205M, V280L, S328F, S499F, S563R, S563L, N578M, V280L/S499F). (C) The residual activity of wild-type (WT) and its mutants after incubation at 45 $^{\circ}$ C for 20 min.

**Figure 2.** Effects of pH and temperature on the activity of WT and its mutants. (A) The optimal reaction pH of WT and its mutants. (B) The optimal reaction temperature of WT and its mutants. (C) The thermostability of WT and the mutants at 45 $^{\circ}$ C. (D) The  $T_m$  of WT and its mutants measured by DSF.



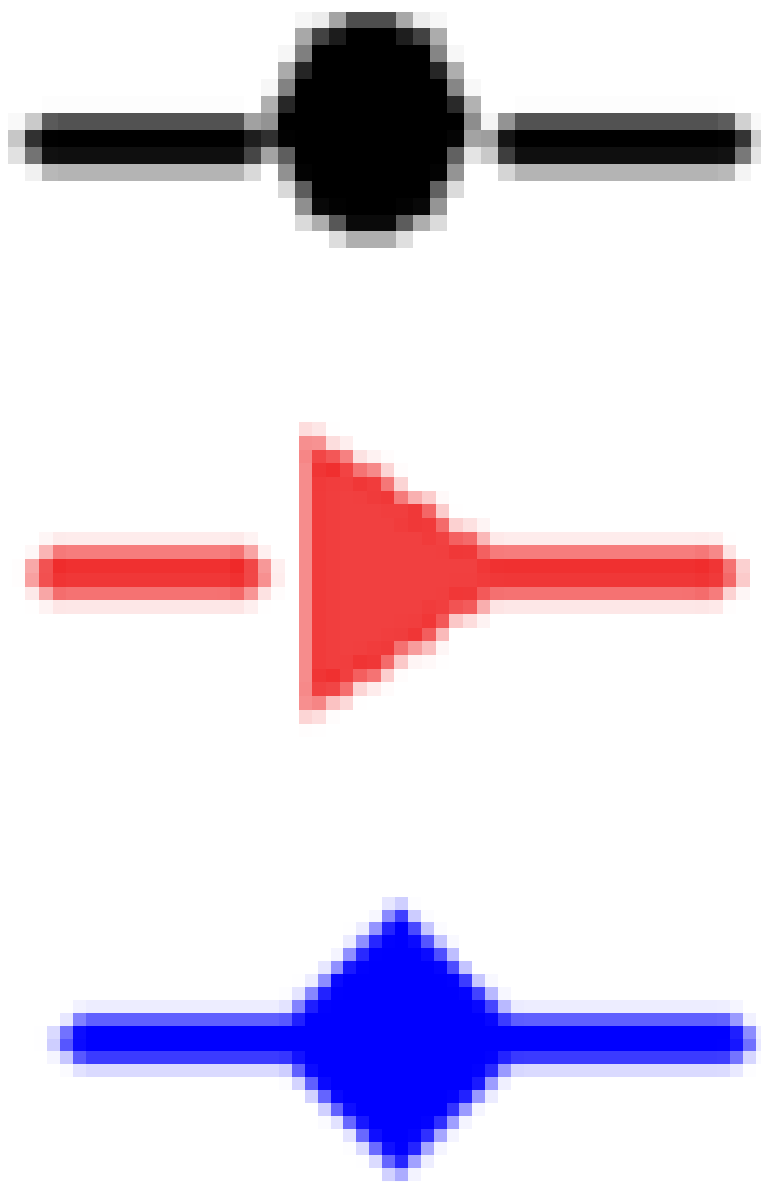


**Figure 3.** Optimization of reaction conditions for whole-cell biotransformation and time course of the production of isomaltulose from sucrose in 5 L fermenter (A) Effect of temperature. (B) Effect of pH. (C) Effect of cell usages. (D) One-batch whole-cell biotransformation. (E) Recyclable synthesis of isomaltulose using a *Corynebacterium glutamicum* whole-cell biocatalyst. (○), residual sucrose (□), glucose production (△) and fructose production (◇).

**Figure 4.** Structure analysis of WT and mutants. (A) V280 was located in  $\alpha$ -helix, which could possibly form two new VDWs with Q329 and W330 in mutant L280 (B) Reddish dashed lines refer to VDWs; (C) Multiple sequence alignment of SIases from different species. Abbreviations are as follows: *Erwinia*

*rhapontici* NCPPB 1578, ERSI; *Pantoea dispersa* UQ68J, PDSI; *Serratia plymuthica* PAMC26656, SPSI; *Enterobacter* sp. FMB-1, ESI; *Raoultella planticola* UQ14S, RPSI; *Pseudomonas mesoacidophila* MX-45, MutB; *Rhizobium* sp. MX-45 (M1E1F7), RSI; *Pectobacterium carotovorum*, PCSI; (E) a new hydrophobic network including F499 and other residues (P24, W339, P495, and L519) was formed in S499(D), the hydrophobic interactions are shown as blue dashed line,  $\pi$ -cation stacked interaction between Trp339 and Phe499 is shown as magentas line; (F) Overall molecular interactions of V280L/S499F;

**Figure 5.** Molecular dynamics simulations. (A) The RMSD values of all backbone atoms for WT and mutants. (B) The RMSF values of each amino acid residue for WT and mutants. Letter I, II represent the amino acid position at site 280, 499, respectively.

**Figure 1**

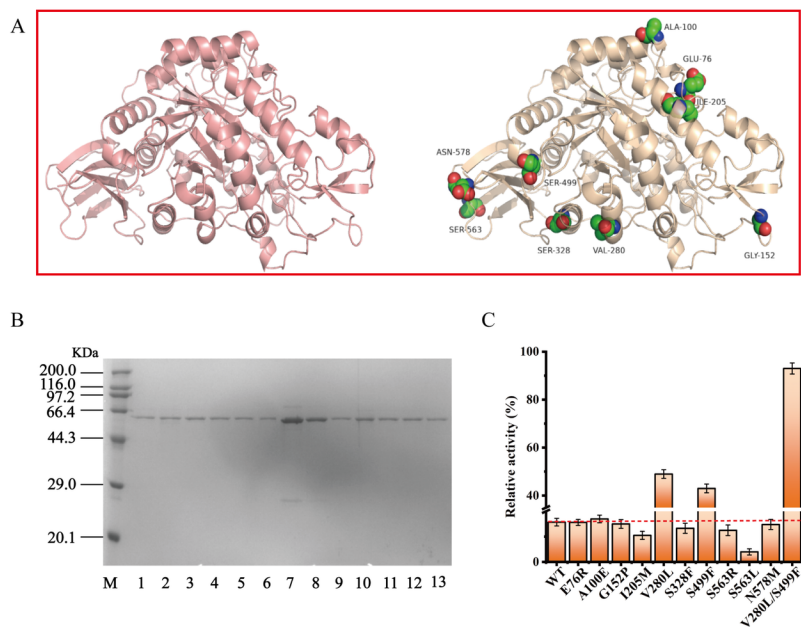


**Figure 2**

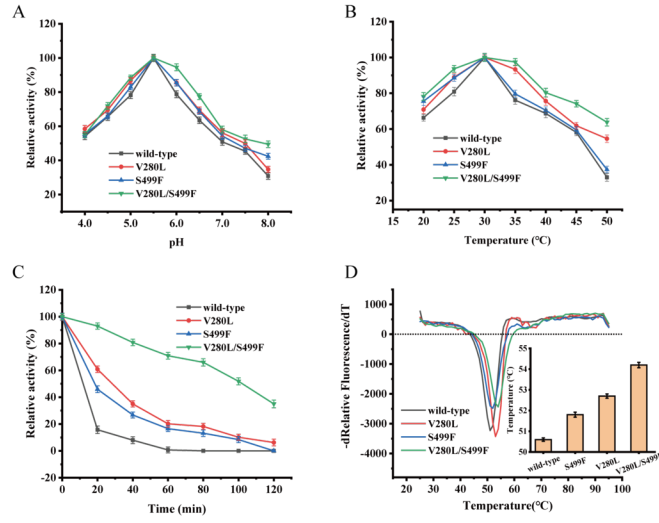


**Figure 3**

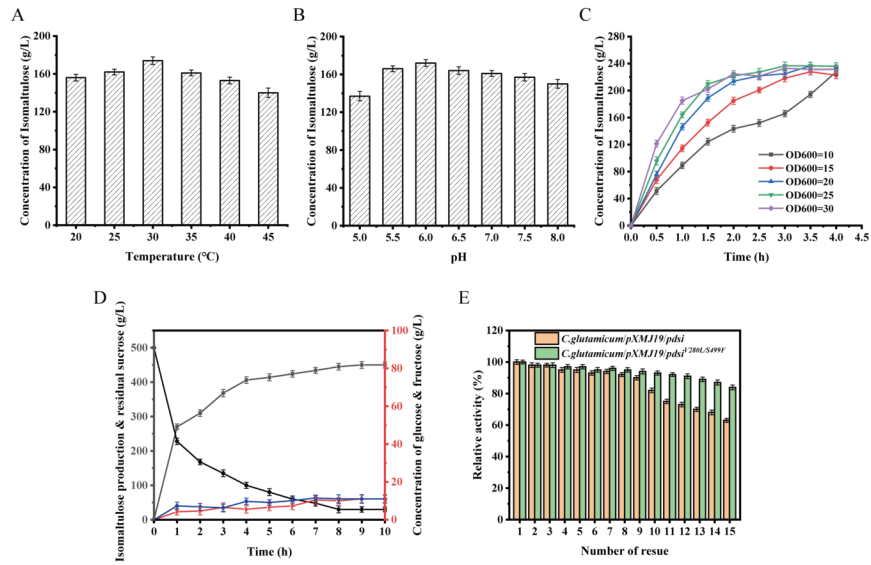


**Figure 4**

